Low RNA translation activity limits the efficacy of hydrodynamic gene transfer to pig liver "in vivo"

Journal:	*Journal of Gene Medicine*
Manuscript ID:	JGM-14-0006.R1
Wiley - Manuscript type:	Research Article
Date Submitted by the Author:	n/a
Complete List of Authors:	Sendra, Luis; Universidad de Valencia, Pharmacology Carreño, Omar; Hospital Universitario y Politécnico La Fe, Unidad de Cirugía Hepatobiliopancreatica y Trasplante Miguel, Antonio; Universidad de Valencia, Farmacologia Montalvá, Eva; Hospital Universitario y Politécnico La Fe, Unidad de Cirugía Hepatobiliopancreatica y Trasplante Herrero, Maria José; Hospital Universitario y Politécnico La Fe, Unidad de Farmacogenética, IIS La Fe, Servicio de Farmacia, Orbis, Francisco; Hospital Universitario y Politécnico La Fe, Unidad de Cirugía Hepatobiliopancreatica y Trasplante Noguera, Inmaculada; Universidad de Valencia, SCSIE, Servicio Central de Soporte a la Investigación Experimental Barettino, Domingo; CSIC, Instituto de Biomedicina de Valencia López, Rafael; Hospital Universitario y Politécnico La Fe, Unidad de Cirugía Hepatobiliopancreatica y Trasplante Alino, Salvador; Universidad Valencia, Farmacologia; Hospital Universitario y Politécnico La Fe, Unidad de Farmacología Clínica, ACM ; Hospital Universitario y Politécnico La Fe, Unidad de Farmacogenética, IIS La Fe, Servicio de Farmacia,
Keywords:	gene - therapy, gene - transfer, plasmid - gene delivery, hepatology, enhanced Green Fluorescent Protein (eGFP)

Low RNA translation activity limits the efficacy of hydrodynamic gene transfer to pig liver "in vivo"

Inefficient RNA translation by hydrodynamic injection

Luis Sendra [1], Omar Carreño [2], Antonio Miguel [1], Eva Montalvá [2], María José Herrero [1,3], Francisco Orbis [2], Inmaculada Noguera [4], Domingo Barettino [5], Rafael López-Andújar [2], Salvador F. Aliño [1,3,6]

[1] Departamento de Farmacologia, Facultad de Medicina, Universidad de Valencia, Valencia, Spain

[2] Unidad de Cirugía Hepatobiliopancreatica y Trasplante, Hospital Universitario y Politécnico La Fe, Valencia, Spain

[3] Unidad de Farmacogenética, IIS La Fe, Servicio de Farmacia, Hospital Universitario y Politécnico La Fe, Valencia, Spain

[4] SCSIE, Servicio Central de Soporte a la Investigación Experimental, Universidad de Valencia, Valencia, Spain

[5] Instituto de Biomedicina de Valencia, CSIC, Valencia, Spain

[6] Unidad de Farmacología Clínica, ACM Hospital Universitario y Politécnico La Fe, Valencia, Spain

Correspondence must be addressed to:

Prof. Salvador F. Aliño and PhD. María José Herrero, Departamento de farmacología, Universidad de Valencia and Instituto de Investigación Sanitaria La Fe, Hospital Universitario y Politécnico La Fe. Valencia, Spain.

E-mail: alino@uv.es and maria.jose.herrero@uv.es

ABSTRACT

Introduction. Hydrodynamic gene delivery has proved an efficient strategy for non-viral gene therapy in the murine liver but it has been less efficient in pigs. The reason for such inefficiency remains unclear. The present study uses a surgical strategy to seal the whole pig liver "in vivo".

Material and Methods. A solution of eGFP DNA was injected under two different venous injection conditions (anterograde and retrograde), employing 10 and 20 ml/s flow rates in each case, with the aim of identifying the best gene transfer conditions. The gene delivery and information decoding steps were evaluated by measuring the eGFP DNA, mRNA and protein copy number 24 hours after transfection. In addition, gold nanoparticles (4 and 15 nm diameter) were retrogradely injected (10 ml/s) to observe, by electron microscopy, the particle ability to access the hepatocyte.

Results. The gene delivery level was higher with anterograde injection whereas the efficacy of gene expression was better with retrograde injection, suggesting differences in the decoding processes. Thus, retrograde injection mediates gene transcription (mRNA copy/cell) equivalent to that of intermediate expression proteins but the mRNA translation was lower than that of rare proteins. Electron microscopy showed that nanoparticles within the hepatocyte were almost exclusively 4 nm in diameter.

Conclusion. Results suggest the low activity of mRNA translation to limit the final efficacy of gene transfer procedure. On the other hand, gold nanoparticles study suggests that elongated DNA conformation could offer advantages to achieve the hepatocyte, since the access of 15 nm particles is very limited.

Keywords: Hydrodynamic, pig, liver, non-viral, gene therapy, nanoparticle.

INTRODUCTION

The hydrodynamic strategy for gene delivery to the liver was first described in the mid-1990s. Budker et al.(1) injected large volumes of naked DNA solution through the portal vein while the hepatic veins were occluded in mice, with resulting high expression of the foreign gene. Zhang G et al.(2) achieved high expressions of foreign genes injecting the DNA solution retrogradely through the hepatic veins. This system was improved upon when injection was carried out through the tail vein (3, 4), resulting in the highest gene expression to that date. The efficiency of this procedure was explained by the inversion of intrahepatic blood flow, due to the porta-cava blood pressure inversion, and the permeability of the liver tissue (5). The high efficiency of this gene delivery strategy made it possible to avoid the use of viral vectors, which could prove more hazardous by inducing adverse immunological reactions and even death (6), and allowed for easier potential clinical application of gene therapy. Nevertheless, a similar model is required for gene delivery in large animals. Although it is safer for gene delivery than viral vector use, hydrodynamic gene delivery is not innocuous, and it has been suggested that the process implies transient hydroporation of the hepatocytes (7), endothelial rupture, massive endocytic vesicles and macropinocytosis (5, 8, 9) and cardiac stress (10). These adverse effects are due to the extreme conditions employed (volume equivalent to 9-10% of total body weight) in small animals. Thus, conditions need to be milder in order to transfer this model to larger animals, and especially to allow potential clinical application in humans. Hydrodynamic gene therapy efficiency depends on the exerted intrahepatic pressure, which is related to the targeted tissue framework (11). Hence, this model had to be modified to achieve a similar pressure level but using a smaller volume of DNA solution. Two different models have been described: lobe-specific infusion of the DNA solution by isolating a single liver lobe, which was tested in rats (7, 12), rabbits (13) and pigs (5, 14, 15, 16, 17); and infusion of the DNA solution to the whole liver through the inferior vena cava - a strategy applied in rats (2, 7, 18), rabbits (13) and pigs (19). The studies in large animals focused on describing and comparing the pressure profiles (15) using different DNA solution infusion and vascular exclusion alternatives, and also reported poor efficiency of hydrodynamic gene transfer to the pig liver. However, the causes of such inefficiency remain unclear. Since the final efficacy of gene expression depends on both gene delivery and the efficiency of the information decoding process, the present study was designed to explore how each step could be limiting the efficiency of the gene transfer process. To date, no detailed molecular biological study has examined “in vivo” gene delivery to the isolated whole pig liver, following the complete genetic decoding process until protein production.

The low efficiency of the system made it important to target the whole liver for gene delivery. Since regional hydrodynamic gene delivery mediated by catheter proved inefficient, it is believed that a surgical procedure to completely isolate the liver is

required (11). We perfused eGFP DNA solution (approximately 1% volume of total body weight) into the whole pig liver subjected to surgical vascular exclusion. The surgical technique for excluding the liver vasculature has recently been described by our group (20) following the work of other authors (16, 17, 19). In the present work, we conceived this surgical procedure as a method to study the gene transfer efficiency and its detailed decoding process of genetic information in “in vivo” large animal model.

The main purpose of this study was to determine which is the most effective way (anterograde or retrograde) for gene transfer, in order to establish the optimum form of injection for future long-term studies employing therapeutic genes. In order to compare the efficacy of the two procedures, we studied each molecular stage of the gene decoding process. Employing this procedure, we compared the functional effects of gene transfer depending on flow direction (anterograde versus retrograde) and rate. It was necessary to evaluate the functional aspects of liver gene transfer at cellular and molecular levels in order to understand the limitations of the procedure. In this sense, we quantified the number of eGFP gene copies in tissue DNA, mRNA and protein as molecular analysis. We then studied the efficiency of gene delivery and its availability for transcription and translation by cell mechanisms. We evaluated the expression of the exogenous gene and the intrinsic activity of transcription and translation of the different alternatives in order to define the optimum perfusion conditions. On the other hand, in order to know the restrictions imposed in crossing biological barriers such as the vascular endothelium and cells membranes, we injected gold nanoparticles (Nps) measuring 4 and 15 nm in diameter, and examined their tissue distribution under the electron microscope.

The mechanism underlying gene delivery after hydrodynamic gene transfer remains to be clarified. Two routes of plasmid entry into the hepatocyte have been suggested: plasma membrane disruption (07) and membrane permeation (14, 05, 21, 22). Previous studies by our group (23) suggest that DNA could access the hepatocyte through a permeation process, since the hydrodynamic injection of 15 nm gold Nps posed an enormous limitation to particle penetration into the hepatocyte. In the present work, we employed Nps measuring 4 and 15 nm in diameter to determine how the membrane structure limits access to the cell as a function of particle diameter.

Our results suggest that DNA, although inefficiently delivered, is widely distributed throughout the liver tissue after hydrodynamic gene transfer, and specific RNA accordingly is also present. In contrast, the presence of the protein is low - suggesting possible blockade of the RNA translation step, probably induced by the hydrodynamic injection. This would be the main factor responsible for the inefficiency of the global gene transfer process. In addition, the ultrastructural study of nanoparticles

distribution in the liver (4 and 15 nm diameter) suggests that strand DNA should be the most probable conformation to successfully achieve the hepatocyte.

RESULTS

Hemodynamic parameters

Hemodynamic parameters were monitored during the entire intervention in order to ensure the safety of the procedure. Blood pressure, oxygen saturation, heart rate and ECG were evaluated. Both portal and cava vein perfusions induced similar changes in pig conditions (Table 1). In sum, both systolic and diastolic blood pressures decreased gradually (approximately 30-50%) when the liver vasculature was completely excluded. The pressure was partially augmented (14-27%) by plasmid injection. The lowest pressure level was reached 5 minutes (time lapse for gene entry to the cell) after injection from 87/61 mmHg (basal) to 42/33 mmHg in retrograde injection and from 98/66 mmHg to 39/29 mmHg in portal perfusion, when blood return had already been blocked for approximately 7 minutes. At that moment, the liver was revascularized and blood pressure recovered in less than 5 minutes, showing no significant differences versus the basal values one minute after revascularization. Contrary to what has been described (10), no relevant changes were detected in the ECG tracing. Oxygen saturation was maintained above 98% during the entire operation. The complete intervention time was less than 60 minutes. Liver vascular exclusion lasted less than 8 minutes, of which 4.5-5 minutes were dedicated to DNA incubation and penetration of the hepatocytes.

Functional analysis

Gene delivery index and apparent efficacy of gene expression

In order to evaluate the delivery efficiency of this strategy, the number of copies of eGFP gene present in the tissue was quantified. Fig. 2 A and B compare eGFP index of gene delivery, expressed as eGFP DNA copies per cell considering the weight (5.4 pg) of pig diploid genome, as described in methods. Figure 2 show the results of the anterograde and retrograde perfusion of eGFP DNA solution at flow rates of 10 (Fig. 2A) and 20 ml/s (Fig. 2B), respectively. The results graphically presented in Figure 2A reflect slightly higher index of gene delivery when perfusion was performed retrogradely at 10 ml/s - significant differences being observed in the LM-1 liver lobe. The gene delivery index employing the 20 ml/s flow rate (Fig. 2B) proved slightly higher with anterograde injection, and significant differences were observed when the whole liver averages were compared. On comparing the results obtained at the two different flow rates, more efficient delivery was seen after injecting at a rate of 10 ml/s ($p<0.05$ in anterograde injection; $p<0.001$ in retrograde injection) but, considering a homogenous distribution, no more than 10% of the cells were transfected with one transgene copy. Three additional exploratory experiments were carried out employing different conditions but not better outcomes were achieved: a) Higher volumes (400 ml) of plasmid solution injected through cava vein at 20 ml/s achieved poor gene delivery indexes of 5×10^{-3} copies of eGFP DNA per cell or even lower and transcription

indexes of 10^0 copies of eGFP mRNA copies per cell; b) 400 ml of plasmid solution injected simultaneously through portal and cava veins at 40 ml/s results in higher indexes of gene delivery (5 x 10^{-1} eGFP DNA copies per cell) although the gene transcription index did not improve the obtained with milder conditions (10^0 copies of eGFP mRNA per cell). Combining the two indexes to calculate the intrinsic activity of transcription (DNA/RNA copies per cell), this was 100-fold lower than the obtained with retrograde perfusion of 200 ml at 20 ml/s; c) Higher flow rates (60 ml/s) and high volumes (600 ml) injected via portal and cava vein simultaneously mediated low indexes of gene delivery (5 x 10^{-2} eGFP DNA copies per cell). The index of gene transcription achieved was not higher than the obtained with milder conditions and these conditions also produced damages in pig liver capsule due to the extreme distension of the organ.

The apparent efficacy of gene expression (eGFP protein/DNA copies per cell) at both 10 ml/s and 20 ml/s showed (Fig. 2 C and D) was higher when perfusion was carried out retrogradely. This efficacy was higher when the milder flow rate was employed - being significantly different when comparing the whole liver average with the 20 ml/s rate in the anterograde direction of flow.

Transcription process: gene transcription index and apparent intrinsic activity of gene transcription

In order to evaluate the efficacy of liver gene delivery, eGFP gene transcription in each of 8 tissue samples obtained per liver was assessed by quantitative RT-PCR, and the data were expressed as the gene transcription index (mRNA copies per cell) and apparent intrinsic activity of gene transcription (mRNA/DNA copies per cell). Results shown in Figures 3 A and B compare the indexes of eGFP gene transcription following the anterograde and retrograde perfusion of DNA solution at a flow rate of 10 or 20 ml/s. Slightly greater gene transcription index was reported (Fig. 3A) with retrograde injection at 10 ml/s (approximately 2-fold) compared with anterograde injection at the same flow rate. A significant difference ($p<0.05$) was observed with the t-test on comparing the whole liver averages. Interestingly, when using 20 ml/s (Fig. 3B), the success of retrograde injection increased - achieving up to 10-fold the transcription index obtained with anterograde perfusion. This difference proved significant ($p<0.001$) in the distal medial left lobe (LM-2) when compared with the same lobe and flow rate in anterograde injection. In a similar way, index of gene transcription following retrograde perfusion at 20 ml/s in LM-2 was approximately 10-fold higher ($p<0.001$) than the transcription observed in the same lobe and flow direction but with the lower 10 ml/s flow rate. The eGFP mRNA copies achieved under the best conditions were comparable to those regarded as normal expression levels of low-intermediate abundance class proteins.

We calculated the apparent intrinsic activity of gene transcription (Fig. 3 C and D) as the copies ratio of eGFP RNA with respect to eGFP DNA copy per cell. This parameter

indicated the availability of the delivered gene for transcription. The intrinsic activity of transcription is apparent, since we cannot know whether each eGFP DNA copy is being transcribed to eGFP RNA. Results demonstrated that greater efficacy occurred with retrograde perfusion when this was carried out at 10 ml/s (Fig. 3C), resulting in a mean intrinsic activity value of approximately 10^3 eGFP RNA copies per gene copy and cell. This index was even significantly higher at 20 ml/s (approximately 2-fold) than at 10 ml/s ($p<0.05$), with the same injection direction. When liver injection was performed retrogradely at 20 ml/s (Fig. 3D), the intrinsic activity of transcription in lobe LM-2 was significantly different ($p<0.05$) to activity in the same liver lobe perfused retrogradely but at 10 ml/s. The mean intrinsic activity value of whole liver retrogradely injected at 10 ml/s was significantly higher ($p<0.05$) than the intrinsic activity achieved in anterogradely injected pigs. This tendency was confirmed in 20 ml/s perfusion, where it proved even more evident ($p<0.001$). Thus, the best conditions for achieving the highest eGFP gene intrinsic activity of transcription were retrograde injection (through the infrahepatic cava vein) of a volume of saline DNA solution equivalent to 1/3 of the liver weight at a flow rate of 20 ml/s. These conditions afforded intrinsic activities comparable to those of intermediate-high abundance class proteins.

Translation process: translation index and intrinsic translation activity

In order to study how the process led to final protein synthesis, eGFP tissue translation was determined by ELISA. We used a special high sensitivity GFP ELISA kit due to the undetectable presence of the protein as evidenced by Western blot and immunohistochemistry (not shown). Data were expressed as translation index (protein molecules per cell) and intrinsic translation activity (eGFP protein molecules/eGFP mRNA copies per cell). Results (Fig. 4) demonstrated relevant differences between the different flow rates and directions employed. At 10 ml/s flow rate, anterograde perfusion showed a higher translation index (Fig. 4 A), liver lobe LM being significantly different ($p<0.05$) from the same lobe perfused retrogradely. Translation index of LM lobe at 10 ml/s proved to be significantly different ($p<0.05$) when compared with 20 ml/s (Fig. 4B) flow rate. When whole liver averages of the translation index were compared, no significant difference was observed between retrograde and anterograde perfusion at the 10 ml/s flow rate; however, a significant difference ($p<0.05$) was found between the 10 and 20 ml/s flow rates when anterograde perfusion was carried out. These results suggest that milder flow conditions and anterograde perfusion could offer advantages for the gene translation process. Intrinsic translation activity (Fig. 4 C and D) was studied for every model to determine the most appropriate conditions for cell gene translation. It was calculated as the ratio of eGFP protein copies with respect to eGFP RNA copies per normalized cell. Results demonstrated a slightly higher efficiency following anterograde perfusion in every liver lobe. When liver injection was performed anterogradely at 10 ml/s (Fig. 4C), the intrinsic activity of mRNA translation in lobe LM was significantly higher than when

employing retrograde perfusion ($p<0.01$) and higher ($p<0.001$) than the achieved with 20 ml/s (Fig. 4D).

When considering the entire liver average, intrinsic translation activity was also significantly ($p<0.01$) higher at the 10 ml/s flow rate than at 20 ml/s with anterograde injection. We also observed an increased ($p<0.01$) translation activity in retrograde perfusion at 10 ml/s versus 20 ml/s. The mean intrinsic gene translation activity value with anterograde perfusion was higher at both 10 ml/s and 20 ml/s than the retrograde injection mean intrinsic translation activity value. The results suggest an inefficient process of eGFP mRNA translation especially when higher rate of injection was employed.

Electron microscopy

The ultrastructural study was made to evaluate the tissue distribution of nanoparticles according to their diameter, in order to know how the natural barriers of the liver tissue limit nanoparticle access to hepatocytes.

Gold nanoparticles measuring 4 and 15 nm in diameter were injected (20 ml/s) into two pig livers, reproducing both the anterograde and the retrograde procedures and tissue distribution of the particles was observed by electron microscopy. The images (Fig. 5) showed an inverse proportional relationship between particle size and penetration capacity. Different cell types were observed. Upper panel shows two hepatocytes in the lower half of the image, macrophagic cells (Kupffer cells) can be seen, too. Details A and B correspond to amplified areas of macrophagic cells, where the particles of 4 and 15 nm diameters can be identified. We systematically found smaller diameter (4 nm) particles (black arrows) within the cytoplasm of the macrophages, while the 15 nm particles were always confined within vesicles. Medium panel shows a hepatocyte with its nucleus (left upper corner) and endothelium (right lower corner). The details in images A, B and C show 4 nm particles located in the cytoplasm close to the nuclear envelope, though no particles were seen to penetrate the nuclear membrane. As expected, the 15 nm particles were also found within vesicles of the endothelial cells (detail D). Most of the hepatocytes contained no large gold nanoparticles. After several observations, we found a single 15 nm particle within a hepatocyte (Lower panel) – suggesting that although penetration of the larger particles can occur, the frequency is very low. We observed no major differences between portal and cava injections in the interaction between the nanoparticles and the tissue.

Liver toxicity

In order to assess possible liver damage as a result of hydrodynamic injection, plasma liver enzymes [aspartate aminotransferase (AST) and alanine aminotransferase (ALT)] were determined 0, 1 and 24 hours after injection. Data can be observed in table 2. The intervention produced an increase in AST levels (125% in portal injection reaching

91.7 ± 16.6 U/l and 80% with cava perfusion until 72.4 ± 29.9 U/l) one hour after injection that was partially reverted (10%) in portal injection and completely reverted in the case of retrograde perfusion 24 hours after injection (82.3 ± 60.7 and 32.4 ± 11.5 U/l, respectively), though the difference between senses of flow did not prove significant. The plasma ALT levels remained unaltered in the evaluated samples. The plasma concentrations reached (< 150 U/l) were not relevant, and in no case were there significant differences between enzyme concentrations.

DISCUSSION

In the present study, different hydrodynamic eGFP gene transfer strategies were employed in a surgically isolated "in vivo" pig liver procedure. The main purpose was to identify the cause of low efficiency of hydrodynamic gene transfer into large animal model (pig) compared with highly efficient gene transfer in mice. The entire liver was completely sealed by ligating all the vasculature except for the vessel used for perfusion, aiming at improving gene transfer efficiency. This methodology achieved low to medium levels of DNA copies and transcript (mRNA), higher flow rates (20 ml/s) succeeding greater DNA and RNA copies into the cell. However, no correlation was observed between mRNA levels and protein expressions. The ultrastructural analysis showed that 4 nm particles reached the hepatocyte, whereas the 15 nm particles showed extremely limited access to the cell, suggesting that small diameter conformations of DNA could offer advantages to achieve the hepatocyte.

Gene therapy has been shown to be a potential clinical alternative. Hydrodynamic gene therapy has achieved therapeutic expression levels of the protein encoded by the gene injected in rodents (1, 2, 3, 4). These results showed gene transfer to be efficient, and indicated that a high intrahepatic pressure is required for delivery. This strategy yielded poor and localized gene expression in large animals (8, 14) when compared to the results obtained in rodents. It was subsequently decided to target the entire liver by injecting through the inferior vena cava. Circulatory block seems to be an essential factor in pigs (15) and humans, as has been demonstrated by our group (23) in watertight human liver segments. It has been reported that liver compliance could be a limiting factor for efficient gene delivery (11). In this regard, it is important to determine the optimum gene transfer conditions of volume and flow rate affording the best outcomes without liver injury. In this sense, the exploratory experiments performed with larger volumes and flow rates actually yielded poorer results, and moreover compromised the safety of the procedure. To date, however, no detailed functional analysis has been made of gene transfer to whole sealed pig liver "in vivo".

We have described a safe surgical "in vivo" watertight liver model recently developed by our group (20), based on previous research (24, 25), which allows us to fully exclude liver vascularization - thereby sealing the entire organ. The time employed for the entire intervention was no more than one hour. The liver ischemia time was less than 8 minutes, and of this period, 5 minutes were used for incubating the DNA solution within the liver. The decrease in blood pressure after vasculature sealing returned to normal values in less than one minute after revascularization, with no relevant changes in the ECG tracing – in contrast to previous findings (19). In addition, there were no significant changes in plasma liver ALT and AST concentrations 24 hours after hydrodynamic injection.

The central idea is that the delivered DNA can show different functionality or cellular availability for transcription, depending on the route of administration (anterograde or retrograde). Accordingly, the DNA molecules that remain outside the cell or are unavailable for transcription account for “quantified delivered DNA”, but are not transcribed. This is the reason why we purpose two parameters for evaluation of the decoding process: total quantification of product (DNA, RNA or protein) as copy number per cell, which is what we call “indexes”; and “intrinsic activities”, which are ratios between different indexes to at least evaluate the molecular apparent availability of DNA or RNA in the transcription and translation steps.

The efficacy of the procedure was evaluated 24 hours after gene transfection in tissue samples of each liver lobe. Results obtained suggested that gene transfer occurred and that eGFP gene was efficiently transcribed in 24 hours. Gene delivery was not efficient, and it must be underscored that its functional potential is not known, since it was not possible to discern whether the quantified eGFP DNA was located within the hepatocyte cytoplasm or in the nuclear compartment. Mild conditions of perfusion led to better delivery outcomes. Retrograde perfusion achieved higher delivery at low flow rates. Anterograde perfusion offered advantages in gene delivery with respect to retrograde perfusion at high flow rates, the difference between average liver values being significant. However, the transcription rate was greater with retrograde sense of flow. We speculate that this could be because the retrograde flow allows the plasmid to access the hepatocyte through membrane zones that facilitate delivery of the exogenous gene with high availability. We do not have an explanation for this fact, though it probably will be necessary to determine how DNA is differentially distributed within the liver, depending on the perfusion protocol employed. The results indicate that 10 % of the hepatocytes could have been transfected with a single gene copy, considering a homogenous gene transfer. The ultrastructural analysis by electron microscopy indicates that vascular and cell membranes are barriers that offer restrictions to crossing, depending on particle size. We observed 4 nm particles within the hepatocytes close to the nuclear membrane, but could not confirm crossing of the latter in any case. Particle size is therefore a restricting factor to be considered in non-viral gene delivery efficiency. Since “in vivo” electroporation (26, 27) has demonstrated efficiency in gene transfer, we could expect that retrograde injection combined with electroporation might result in increased efficacy of liver gene delivery with potential therapeutic interest.

We evaluated the eGFP tissue transcription index in order to determine whether gene transfer was effective. Transcription of the eGFP gene (eGFP RNA copies) also was slightly greater in retrograde gene perfusion at 10 ml/s versus anterograde injection. This difference was further increased when injection was carried out at 20 ml/s. These data suggest that DNA delivered by retrograde injection could result more available for hepatocyte transcription, achieving gene expression levels comparable to those

obtained under normal conditions for low-intermediate abundance class proteins (5-400 RNA copies per cell). This could be due to the anadromous sense of flow, as it entered through the endocytic vesicles and augmented membrane permeation. To establish the transcription efficiency of the delivered DNA, we evaluated the intrinsic gene transcription activity (28), which describes gene availability for transcription and is expressed as the number of RNA copies produced per copy of DNA and cell. To calculate this value, we considered a pig haploid genome weight of 2.7 pg (29) and an average of 20 pg total RNA per mammalian cell (30, 21). Results demonstrated considerably greater efficacy when delivery was performed through the cava vein than through portal vein injection – thus supporting the idea that DNA delivered through retrograde injection offers functional advantages for transcription with respect to DNA administered via anterograde injection. The intrinsic transcription activity achieved was similar to that observed for endogenous intermediate-high abundance class (30, 31) proteins.

Unexpectedly, we found a low amount of eGFP protein in the tissue which limited its observation with other procedures different from the high sensitivity ELISA kit, such as Western blot or immunohistochemistry, even when using a procedure previously shown to be successful in our laboratory (23, 33). We consider that this is not due to the gene construct or to the short period of time elapsed after transfection, since in other models (cell culture, human liver segments and pig heart) it has been efficiently expressed 24 hours after transfection, as demonstrated by fluorescence (34). The average copy number of a protein per hepatocyte is around 20,000 for those considered rare, versus $5x10^8$ for very abundant proteins such as actin (31). We detected around 10^1-10^3 copies of eGFP protein per cell - this concentration being lower than that of rare proteins. As mentioned above, the low index of DNA delivery (0.1 copy per cell) resulted in low-intermediate gene transcription efficacy (approximately 20 mRNA copies per cell). Despite this efficiency of transcription, we found unexpectedly very low amounts of eGFP protein, lower than the rare proteins expression rate - suggesting that the hydrodynamic process induces negative effects upon hepatocyte gene translation. Some authors (35) have reported that high volume hydrodynamic gene transfer could induce an inflammatory response which could inhibit gene expression, though the relationship has not been clearly established. Our previous attempts to evaluate the effect of the expression of inflammatory molecules in transgene expression in small animals employing DNA arrays (36, 37) failed to identify a direct influence. Hydrodynamic injection of saline solution (2 ml) with and without pTG plasmid (20 µg/ml) did not induce changes in general protein expression two and 10 days after injection. Moreover, in our experiments, no significant inflammation or liver injury has been detected, as reflected by the low transaminase levels. In this respect, it has been described that endoplasmic reticulum stress is a checkpoint in protein biosynthesis (38) that could activate signals involved in blocking the translation of mRNA (39). This delivery rate should be improved but it was higher

than that observed in mice transfected in optimum conditions but in this latter animal model the protein translation index in tissue was more than 1,000-fold higher (data not shown). We thus raise the question of whether similar stress effects could be mediated by retrograde hydrodynamic injection, since an increased endocytic process was previously reported (5, 14) by this gene transfer procedure in both mouse and pig models. These effects could trigger the sequestration of exogenous mRNA, reducing its functionality and/or the inhibition of factors involved in mRNA translation (40). However, little is known of the mechanism underlying this effect or of how the sense of flow or exogenous DNA is involved in this process. Based on our results, it appears that the amount of delivered DNA is not the main factor for efficient gene expression. However, our results do not exclude that anterograde injection may have some inhibitory effects upon transcription. Whereas gene transcription and its intrinsic activity increased with the flow rate, the corresponding data referred to gene translation and intrinsic translation activity remained constant or even decreased (mainly in retrograde injection).

These data suggest that, to achieve increases in gene expression levels, not only higher gene delivery efficiency is required, but also circumvent the negative effect that hydrodynamic delivery could induce on protein translation. Future long-term experiments will allow us to determine whether the procedure can affect the kinetics of transgene expression over time. Ultrastructural analyses, in turn suggest that the size and conformation of the injected plasmid could be a limit the hepatocyte access. The greater penetration capacity of DNA molecules with a size similar to that of the Nps employed suggests that DNA could access the cell following a permeation process without membrane disruption. Therefore, we conclude that hydrodynamic gene transfer to surgically isolated pig liver “in vivo” is a safe procedure that offers potential efficacy in relation to gene transfer if sufficient translation efficacy can be achieved to be translated into human clinic.

MATERIAL AND METHODS

Animals

Female pigs (18-23 kg) were obtained from a farm supplying the Health Research Institute (IIS) of La Fe Hospital (Valencia, Spain), and were housed in individual pigsties. The experiments were approved by the Animal Biological Research Ethics Committee of the Hospital.

Anesthesia was induced with ketamine (Imalgene 100, Merial France; 5-10 mg/kg, im), midazolam (Hospira 1 mg/ml, Madrid, Spain; 0.3 mg/kg, im) and propofol (Lipuro 2%, Braun, Melsungen, Germany; 4-6 mg/kg, iv), and was maintained with sevoflurane (Sevorane, Abbott laboratories, Madrid, Spain; 2.5%, inhalatory route). Muscle relaxation was induced with vecuronium bromide (Norcuron 10 mg; 0.08 mg/kg, iv). Morphine (0.4 mg/kg, iv) was administered for intraoperative analgesia, and buprenorphine (Buprex, Schering-Plough, Madrid, Spain; 0.02 mg/kg, iv) for postoperative analgesia. Vital functions were monitored throughout the intervention. The pigs were sacrificed 24 hours after the operation using potassium chloride (Braun 2 mEq, 20 mEq, iv), after sedation. Blood samples (2 ml) were collected from an ear vein at 0 h (before plasmid injection), 1 h after injection, and 24 h after injection before sacrifice. The liver was extracted, and representative tissue samples of each lobule were collected for further analysis.

Surgical equipment

Surgical laparotomy equipment, vessel loops (DEVON TM COVIDIEN) for referencing vascular structures, and clamps were required. We used three types of sutures: BiosynTM 5/0 (COVIDIEN) for vena cava, ProleneTM 6/0 (ETHICON) for portal vein, and DexonTM 2/0 (COVIDIEN) for closing the abdominal wall. Staples were used to close the skin.

Surgical technique

The pigs were anesthetized. A catheter was placed in the external jugular vein for infusion and blood sampling, while another catheter was placed in the femoral artery for monitoring blood pressure. A complete midline laparotomy was carried out, exposing all the abdominal organs. The extrapancreatic portal vein was exposed and encircled with one or two vessel loops, depending on the cannulation model involved. The hepatic artery was referenced with a silk ligature. The inferior vena cava above the renal veins was dissected and referenced with one or two vessel loops, depending on the cannulation model used. The suprahepatic vena cava was encircled with a vessel loop.

This surgical technique allowed us to establish two models of perfusion in total hepatic vascular occlusion. In model 1, only perfusion through the vena cava was performed, while in model 2 only the portal vein was perfused.

The clamping sequence was as follows: first the hepatic artery, then the portal vein and finally the infrahepatic vena cava, to interrupt hepatic inflow. The suprahepatic vena cava was clamped last, to secure total hepatic vascular exclusion. In model 1 the portal vein was clamped, and only a longitudinal incision was made on the anterior surface of the cava vein to insert the perfusion cannula.

In model 2, the process was the same as in model 1 but with clamping of the vena cava and perfusion through the portal vein.

After solution perfusion, the liver was kept under total vascular exclusion for no more than 5 minutes to allow gene penetration into the cell nuclei. During this time, the incisions of the veins were sutured. Progressive declamping was carried out in the reverse sequence, first allowing liver outflow and finally inflow through the portal and cava veins. The animals were sacrificed after 24 hours in order to carry out the molecular analysis of the liver samples. This model required a short period of time (no more than one hour). The vital signs were monitored continuously to ensure the safety of the procedure.

Plasmid construction

The plasmid p3c-eGFP (6.45 kb), containing the enhanced green fluorescent protein complementary DNA (cDNA) driven by pCMV (cytomegalovirus) promoter, was constructed by cloning eGFP into the *HindIII* site of pcDNA3 (Invitrogen, Barcelona, Spain), excised from peGFP-N1 (4.7 kb) plasmid vector (Clontech Laboratories, Saint-Germain-en-Laye, France).

"In vivo" gene transfer to pig liver

The 11F catheter was placed in the cava or portal vein for gene transfer. After catheter fixation with needle and thread, a solution containing the eGFP plasmid (20 μg/ml) was injected with a high volume pump at different flow rates and a volume of 200 ml (approximately 1/3 of the organ weight according to body weight). Flow rates employed were 10 and 20 ml/s (anterograde/retrovenous). Additional exploratory conditions were employed: 400 ml at 20 ml/s through cava vein; 400 ml at 40 ml/s through portal and cava vein simultaneously employing a Y-connection; and 600 ml at 60 ml/s anterograde and retrovenous, simultaneously. Representative tissue samples were obtained from each lobe. Tissue samples < 1 mm in thickness were subsequently collected under sterile conditions and stabilized in RNAlater solution (Ambion).

Samples were removed one day after collection and processed for molecular analysis to evaluate gene transcription and its efficacy.

Quantitative analysis of DNA and RNA by real time PCR and RT-PCR

Liver tissue samples (8 per liver corresponding to proximal and distal areas of each major liver lobe) were cut into small pieces and homogenized in RLT buffer (Qiagen®, Barcelona, Spain) with an Ultra-Turrax homogenizer (Hielscher Ultrasonics GmbH, Teltow, Germany). Further purification with the RNeasy midi kit (Qiagen®, Barcelona, Spain) was performed before spectrophotometric quantification. RNA retrotranscription to cDNA was carried out using 1 μg total RNA (DNA free), random hexamers and a High Capacity cDNA Archive Kit (Applied Biosystems). For quantitative real-time qPCR, power SYBR GreenPCR master mix (Applied Biosystems) was employed according to the instructions of the manufacturer.

Oligonucleotides were designed with Primer Express software (Applied Biosystems).

The specific primers for eGFP were:

Fw: 5'-GTAAACGGCCACAAGTTCAGC-3', Tm: 53.9 ºC

Rv: 5'-TGGTGCAGATGAACTTCAGGG-3', Tm: 54.9 ºC

The precise amount of RNA (based on optical density readings) and its quality (lack of degradation) were normalized with respect to an endogenous control gene (glyceraldehyde 3-phosphate dehydrogenase (GAPDH)). Quantitative data were calculated as the number of RNA copies on a regression curve which was plotted employing the injected plasmid containing the eGFP gene. A standard curve was prepared with the same transferred plasmid, performing serial dilution 1/10 from 1 to 1,000,000 gene copies. The curve showed linearity from 100 copies to 1,000,000 copies, and each sample result was in this range. The total amount of DNA in the PCR was approximately 1 μg per sample. The total amount of RNA (cDNA) in the PCR was 100 ng per sample. The theoretical sensitivity of the procedure for eGFP DNA detection was 0.5 copy per 1,000 cells, which means > 10-3 eGFP DNA copies per cell. Since the plasmid contains eGFP cDNA, the curve served for both DNA (delivery) and RNA (transcription). The theoretical sensitivity of the procedure for RNA detection was 0.02 molecules of eGFP RNA per cell (20 eGFP RNA molecules per 1,000 cells). Data plotting was performed using GraphPad Prism 5 (GraphPad Software, San Diego, CA, USA).

The data have been expressed as copy number of eGFP DNA, RNA or protein per cell. To calculate the parameters related with delivery and decoding steps of transcription and translation, we took into consideration the following information: a) for gene delivery study, we are considering 5.4 pg as the weight of the pig diploid genome (NCBI

Database); b) for gene transcription evaluation, we consider 20 pg as the average content of RNA per cell in a mammalian hepatocyte (Alberts et al. 2002, Brown et al. 2002); c) for mRNA translation, 0.5 ng was considered the amount of protein per cell (Alberts et al. 2002, Brown et al. 2002). According to these considerations, the following parameters per cell were calculated:

Indexes: indicate the total amount of eGFP DNA, RNA or protein per normalized cell, respectively. These parameters were determined by direct quantification and transformed to "number of molecules per cell" according to the above mentioned criteria. These indexes have quantitative value but do not indicate the quality of the procedure. For instance, the index of gene transcription per cell indicates the number of specific mRNA copies per cell, but does not indicate how many DNA copies were required.

- Index of gene delivery: (nº eGFP DNA copies/pg of total DNA) * 5.4

- Index of gene transcription: (nº eGFP mRNA copies/pg of total RNA) * 20

- Index of gene translation: (nº eGFP protein molecules/pg of total protein) * 500

Intrinsic activities: these parameters are ratios between different indexes for at least evaluating the molecular apparent availability in each step of the decoding process. These parameters refer mainly to the apparent quality of the procedure and to molecular availability. The term "apparent" was used, since it is not possible to know whether all the DNA and RNA copies are available for transcription and translation, respectively.

- Apparent intrinsic activity of gene expression: [(nº eGFP protein molecules/pg of total protein) * 500]/[(nº eGFP DNA copies/pg of total DNA) * 5.4]

- Apparent intrinsic activity of gene transcription: [(nº eGFP mRNA copies/pg of total RNA) * 20]/[(nº eGFP DNA copies/pg of total DNA) * 5.4]

- Apparent intrinsic activity of gene translation: [(nº eGFP protein molecules/pg of total protein) * 500]/[(nº eGFP mRNA copies/pg of total RNA) * 20]

Although previous studies have been carried out to calculate these parameters, the exact a.i.a. values for reference genes are not available in the databases. However, some of them could be calculated, since they have been classified as high, intermediate or low producers of RNA (5-15, 20-400, > 104 copies of RNA per cell, respectively; ref. 30, 31) and protein (102-103, 103-105, >105 copies of protein per cell, respectively. The quantitative proteome of a human cell line (Martin Beck et al. 2011) and the DNA copy number per cell are known. For example, we can obtain the following mean values for actin gene (high producer) per cell, in a typical mammalian hepatocyte: two DNA copies, 103 RNA copies and 108 copies of protein.

eGFP Protein determination

Liver tissue samples (8 per liver, corresponding to different areas) were homogenized with an Ultra-Turrax homogenizer, and protein was purified by sequential precipitation employing cold acetone 80% and ethanol 70%. Protein extract was suspended in radioimmune precipitation assay buffer (50 mm HEPES pH 7.4, 150 mm NaCl, 1 mm EGTA, 10 mm NaF, 0.5% Nonidet P-40, 1 mm sodium orthovanadate, 10 µg/ml leupeptin, 10 µg/ml aprotinin, 100 µm PMSF). The protein content was determined with the NanoOrange protein quantitation kit (Invitrogen, CA, USA). Western blot was performed as described elsewhere (41). Antibodies against GFP were obtained from Abcam (Ab290, Cambridge, MA, USA). Horseradish peroxidase-conjugated secondary antibodies were obtained from GE Healthcare. eGFP protein quantitation was carried out with ELISA. Protein samples were analyzed employing a high sensitivity ELISA kit, as Western blot demonstrated very low amounts of protein. The ELISA kit was obtained from Cell Biolabs (akr-121, San Diego, CA, USA). ELISA was performed with this high sensitivity commercial kit according to the instructions of the manufacturer. Antibodies and recombinant GFP standard for curve preparation were included in the kit. In brief, samples were incubated in anti-GFP antibody coated plate and then 1/1000 diluted biotinylated anti-GFP antibody was added for incubation. After corresponding washes, 1/2000 diluted streptavidin-enzyme conjugate was added. After incubation and washes, the substrate solution was added and the absorbance read at 450 nm. The standard curve was linear from 0 to 250 pg/ml, with a correlation coefficient > 0.99. Sample results were inside the standard curve value range in each case. Results were obtained as pg/ml and were converted to copy number assuming a molecular weight of 27 kDa for eGFP protein, and considering the amount of total protein calculated in each individual sample.

Data analysis

Data were graphically represented and statistically analyzed by employing the Prism Graphpad software. The statistical analyses performed were: two-way ANOVA to compare the effects of flow rate and direction in the efficiency of delivery, transcription and translation among the different groups. Although biological samples rarely present Gaussian distribution we employed a parametric analysis (ANOVA) because we are comparing 24 samples (large sample) per group. In these cases the distribution is considered approximately Gaussian and the ANOVA test is routinely used. In contrast, when comparing the group averages (flow rate and direction independently), we had to use nonparametric test with Mann-Whitney correction since these tests are the most appropriate for biological samples not following a Gaussian distribution when sample is small.

Liver toxicity

Peripheral blood samples were taken at different time points: 0 h, before injection; 1 h after injection; and 24 h after injection, before sacrifice. Main liver enzymes (aspartate aminotransferase (AST) and alanine aminotransferase (ALT)) were quantified to determine possible toxic effects of the intervention upon the liver.

Gold nanoparticle synthesis

All chemicals were purchased from Sigma-Aldrich (Madrid, Spain) and used as received, without further purification. Gold nanoparticles were synthesized following a modification of the Turkevich method (42). Typically, 0.4 g of HAuCl4.3H2O was dissolved in 90 ml of water in a two-neck round flask (1.3 mM HAuCl4). The resulting solution was heated to boiling and refluxed. Then, 9 ml of a 47.2 mM sodium citrate solution (0.125 g sodium citrate in 9 ml water) was preheated and quickly added. The solution turned from yellow to black and to deep red. After the color changed, the solution was refluxed for 20 min. Then, the heater was turned off and the solution was stirred until it reached room temperature. The resulting solution was diluted with water to a final volume of 500 ml. Gold nanoparticles were characterized by transmission electron microscopy (TEM) (Jeol 1010, Tokyo, Japan). The average diameter and the size distribution of the gold nanoparticles were determined from TEM images by counting at least 300 nanoparticles using Image Pro Plus software from Media Cybernetics (Bethesda, MD, USA).

Transmission electron microscopy

Pig livers (n=2) were injected (volume 200 ml) through the catheter placed in the cava (n=1) or in the portal vein (n=1) with a solution of citrate buffer containing 10^{12} gold particles (4 nm and 15 nm in diameter) per ml to study the liver distribution of gold nanoparticles after injection, depending on the injection sense of flow and the size of the particles. Then, in both cases small tissue pieces from different liver areas were removed and immersed in phosphate Sørensen buffer solution (pH 7.4) containing 2.5% glutaraldehyde. For TEM, multiple 1-mm^3 pieces of liver were routinely processed and embedded in Epoxy resin. Ultrathin sections, stained with uranyl acetate, were examined under a Jeol JEM-1010 electron microscope. The sections were not stained with lead citrate as usual, because it could interfere with the gold nanoparticles and make their detection very difficult.

ACKNOWLEDGEMENTS

We thank Dr. Rafael Abargues from the Instituto de Ciencia de Materiales, Universidad de Valencia (Valencia, Spain) for synthesizing and providing the gold nanoparticles for the ultrastructural analysis.

This study has been supported by projects from the Spanish Ministry of Science (SAF2011-27002) and the *Generalitat Valenciana* (AP 151-11).

CONFLICTS OF INTEREST

The authors declare that **No competing financial interests exist**.

REFERENCES

(1) Budker V, Zhang G, Knechtle S, Wolff JA. Naked DNA delivered intraportally expresses efficiently in hepatocytes. Gene Therapy 1996; 3: 593–598.

(2) Zhang G, Vargo D, Budker V, Armstrong N, Knechtle S, Wolff JA. Expression of naked plasmid DNA injected into the afferent and efferent vessels of rodent and dog livers. Hum Gene Ther 1997; 8: 1763–1772.

(3) Liu F, Song Y, Liu D. Hydrodynamics-based transfection in animals by systemic administration of plasmid DNA. Gene Therapy 1999; 6: 1258–1266.

(4) Zhang G, Budker V, Wolff JA. High levels of foreign gene expression in hepatocytes after tail vein injections of naked plasmid DNA. Hum Gene Ther 1999; 10: 1735–1737

(5) Crespo A, Peydro A, Dasi F, Benet M, Calvete JJ, Revert F et al. Hydrodynamic liver gene transfer mechanism involves transient sinusoidal blood stasis and massive hepatocyte endocytic vesicles. Gene Therapy 2005; 12: 927–935.

(6) Kay MA, Glorioso JC, Naldini L. Viral vectors for gene therapy: the art of turning infectious agents into vehicles of therapeutics. Nat Med. 2001 Jan;7(1):33-40.

(7) Zhang G, Gao X, Song YK, Vollmer R, Stolz DB, Gasiorowski JZ et al. Hydroporation as the mechanism of hydrodynamic delivery. Gene Therapy 2004; 11: 675–682.

(8) Herrero MJ, Dasi F, Noguera I, Sanchez M, Moret I, Sanmartin I et al. Mouse and pig nonviral liver gene therapy: success and trials. Gene Ther Mol Biol 2005; 9: 169–180.

(9) Suda T, Gao X, Stolz DB, Liu D. Structural impact of hydrodynamic injection on mouse liver. Gene Therapy 2007; 14: 129–137.

(10) Sawyer GJ, Dong X, Whitehorne M, Grehan A, Seddon M, Shah AM, Zhang X and Fabre JW. Cardiovascular function following acute volume overload for hydrodynamic gene delivery to the liver. Gene Ther. 2007 Aug; 14(16):1208-17.

(11) Sawyer GJ, Rela M, Davenport M, Whitehorne M, Zhang X, Fabre JW. Hydrodynamic gene delivery to the liver: theoretical and practical issues for clinical application. Curr Gene Ther. 2009 Apr;9(2):128-35.

(12) Zhang X, Collins L, Sawyer GJ, Dong X, Qiu Y, Fabre JW. In vivo gene delivery via portal vein and bile duct to individual lobes of the rat liver using a polylysine-based nonviral DNA vector in combination with chloroquine. Hum Gene Ther 2001; 12: 2179–2190.

(13) Eastman SJ, Baskin KM, Hodges BL, Chu Q, Gates A, Dreusicke R et al. Development of catheter-based procedures for transducing the isolated rabbit liver with plasmid DNA. Hum Gene Ther 2002; 13: 2065–2077.

(14) Aliño SF, Herrero MJ, Noguera I, Dasí F, Sánchez M. Pig liver gene therapy by noninvasive interventionist catheterism. Gene Therapy 2007; 14: 334–343.

(15) Fabre JW, Whitehorne M, Grehan A, Sawyer GJ, Zhang X, Davenport M, Rela M. Critical, physiological and surgical considerations for hydrodynamic pressurization of individual segments of the pig liver.Hum Gene Ther. 2011 Jul;22(7):879-87.

(16) Kamimura K, Suda T, Xu W, Zhang G, Liu D. Image-guided, Lobe-specific Hydrodynamic Gene Delivery to Swine Liver. Mol Ther. 2009 Mar; 17(3):491-9.

(17) Yoshino H, Hashizume K, Kobayashi E. Naked plasmid DNA transfer to the porcine liver using rapid injection with large volume. Gene Therapy 2006; 13: 1696–1702.

(18) Sawyer GJ, Zhang X, Fabre JW. Technical requirements for effective regional hydrodynamic gene delivery to the left lateral lobe of the rat liver. Gene Therapy 2010; 17:560–564.

(19) Fabre JW, Grehan A, Whiterhorne M, Sawyer GJ, Dong X, Salehi S et al. Hydrodynamic gene delivery to the pig liver via an isolated segment of the inferior vena cava. Gene Therapy 2008; 15: 452–462.

(20) Carreño O, Sendra L, Montalvá E, Miguel A, Orbis F, Herrero MJ, Noguera I, Aliño SF, López Andújar R. A Surgical Model for Isolating the Pig Liver in vivo for Gene Therapy. European Surgical Research 2013. DOI: 10.1159/000351339

(21) Sebestyén MG, Budker VG, Budker T, Subbotin VM, Zhang G, Monahan SD et al. Mechanism of plasmid delivery by hydrodynamic tail vein injection. I. Hepatocyte uptake of various molecules. J Gene Med 2006; 8: 852–873.

(22) Suda T, Gao X, Stolz DB, Liu D. Structural impact of hydrodynamic injection on mouse liver. Gene Therapy 2007; 14: 129–137.

(23) Herrero MJ, Sabater L, Guenechea G, Sendra L, Montilla AI, Abargues R, Navarro V and Aliño SF. DNA delivery to 'ex vivo' human liver segments. Gene Ther. 2012 May; 19(5):504-12.

(24) de Groot GH, Reuvers CB, Schalm SW, Boks AL, Terpstra OT, Jeekel H, ten Kate F, Bruinvels J. A reproducible model of acute hepatic failure by transient ischemia in the pig. J Surg Res. 1987 Jan;42(1):92-100

(25) Lee KU, Zheng LX, Cho YB, Kim KH, Ha J, Suh KS, Jung SE. An experimental animal model of fulminant hepatic failure in pigs. J Korean Med Sci. 2005 Jun;20(3):427-32

(26) Li S. Electroporation gene therapy. Preface. Methods Mol Biol. 2008; 423:v-vii.

(27) Heller LC, Heller R. Electroporation gene therapy preclinical and clinical trials for melanoma. Curr Gene Ther. 2010 Aug; 10(4):312-7.

(28) Balagopal V. and Parker R. Polysomes, P bodies and Stress granules: States and Fates of Eukaryotic mRNAs. Curr Opin Cell Biol. 2009 Jun; 21(3):403-8. doi: 10.1016/j.ceb.2009.03.005.

(29) NCBI Genome Database. http://www.ncbi.nlm.nih.gov/genome/84. (accessed on December 2012).

(30) Molecular biology of the cell, 4th edition. Alberts B, Johnson A, Lewis J, et al. New York: Garland Science; 2002. Chapter 6: From DNA to RNA. Available from: www.ncbi.nlm.nih.gov/books/NBK26887

(31) Genomes, 2nd Edition. Brown TA. Oxford: Wiley-Liss. 2002. Chapter 3: Transcriptomes and Genomes. Available from: www.ncbi.nlm.nih.gov/books/NBK21121

(32) Lodish H, Berk A, Zipursky SL, et al. Molecular Cell Biology. 4th edition. Chapter 3. New York: W. H. Freeman; 2000

(33) Aliño SF, Herrero MJ, Bodí V, Noguera I, Mainar L, Dasí F, Sempere A, Sánchez M, Díaz A, Sabater L, Lledó S. Naked DNA delivery to whole pig cardiac tissue by coronary sinus retrograde injection employing non-invasive catheterization. J Gene Med 2010; 12: 920–926.

(34) Aliño SF,* Escrig E, Revert F, M. Guillem VM and Crespo A. Pharmacodynamic approach to study the gene transfer process employing non-viral vectors. Biochem Pharmacol. 2000 Dec 15;60(12):1845-53.

(35)Rácz Z, Godó, Révész C, Hamar P. Immune activation and target organ damage are Consequences of hydrodynamic treatment but not delivery of naked siRNAs in mice. Nucleic Acid Ther 2011; 21(3):215-24.

(36) Herrero MJ, Monleon D, Morales JM, Mata M, Serna E and Aliño SF. Microarray analysis of gene expression changes in mouse liver induced by hydrodynamic DNA injection. Curr. Top. Gen. 2010; Vol. 4: 43-54.

(37)Herrero MJ, Monleon D, Morales JM, Mata M, Serna E, Aliño SF. Analysis of Metabolic and Gene Expression Changes after Hydrodynamic DNA Injection into Mouse Liver. Biol. Pharm. Bull 2011; 34(1) 167—172.

(38)Harding HP, Calfon M, Urano F, Novoa I, Ron D. Transcriptional and translational control in the Mammalian unfolded protein response. Ann. Rev. Cell. Dev. Biol 2002; 18:575-99

(39)Walter, P; Ron, D. The Unfolded Protein Response: From Stress Pathway to Homeostatic Regulation. Science. 2011; 334:1081-1086.

(40)Cargnello M, Tcherkezian J, Dorn JF Huttlin E, Maddox P Gygi S and Roux P. Phosphorylation of the Eukaryotic Translation Initiation Factor 4ETransporter (4E-T) by c-Jun N-Terminal Kinase Promotes Stress-Dependent P-Body Assembly. Mol Cell Biol. 2012 Nov;32(22):4572-84. doi: 10.1128/MCB.00544-12.

(41)Masiá S., Alvarez S., de Lera A. R., Barettino D. (2007) Mol. Endocrinol. 21, 2391–2402.

(42)Kimling J, Maier M, Okenve B, Kotaidis V, Ballot H, Plech A. Turkevich method for gold nanoparticle synthesis revisited. J Phys Chem 2006; 110: 157–160.

Tables and figure legends

Table 1. Hemodynamic parameters during the intervention. Hemodynamic parameters (systolic and diastolic blood pressure) and other vital signs (heart rate, ECG and oxygen saturation) were monitored during the entire surgical intervention. Data in the table represent the animal conditions at critical points of the procedure. Significant differences were detected in blood pressures at different time points. *=p<0.05; **=p<0.01 and ***=p<0.001 when blood pressures are compared to basal blood pressure. To evaluate the recovery time of hemodynamic conditions, blood pressure values after revascularization were compared with the lowest values of these parameters recorded at the end of plasmid incubation. ‡=p<0.05; ‡‡=p<0.01; ‡‡‡=p<0.001 when compared with pre-reperfusion blood pressure. No significant differences between portal and cava vein injection were detected.

Table 2. Liver injury: levels of AST and ALT. The table shows AST (aspartate aminotransferase) and ALT (alanine aminotransferase) levels at 0 (basal level), 1 and 24 hours post injection. Normal values for AST: 15-55 I/U; normal values for ALT 21-46 I/U.

Figure 1. Surgical procedure. Schematic representation of the surgical procedure and the site of sampling. Laparotomy was performed to reference the liver vasculature. Once the vessels were referenced, suprahepatic cava vein, hepatic artery and portal or infrahepatic cava vein (depending on perfusion direction, retrograde or anterograde, respectively) were clamped to fully seal the entire liver. Then, injection was performed through the chosen vein. Tissue sampling zones are represented. The name indicates the location. First letter: R=right, L=left; second letter: M=medial, L=lateral; number: 1=proximal, 2=distal. Sampling was carried out 24 hours after injection. **Figure 2. Gene delivery index and intrinsic gene expression activity.** Two hundred ml of DNA saline solution containing the eGFP gene (20 µg/ml) was injected anterogradely (portal vein) or retrogradely (cava vein) into the liver at different flow rates (10 and 20 ml/s). Fig. 2A represents gene delivery when perfusion was carried out at 10 ml/s, Fig. 2B represents gene delivery when perfusion was carried out at 20 ml/s. Gene delivery is indicated as eGFP copies of DNA per cell calculated by qPCR, considering a pig diploid genome weight of 5.4 pg. Delivery corresponding to each liver lobe is represented. Portal vein injection achieved similar gene delivery at 10 ml/s and slightly higher gene delivery at 20 ml/s, significant difference was observed for LM-1 lobe retrogradely injected at 10 ml/s (marked with ++, p<0.05) (two-way ANOVA and Bonferroni post hoc testing). Delivery index mean values of every perfusion condition were compared statistically by nonparametric (Mann-Whitney correction) t test and results showed significant differences between different flow rates and same flow direction (a, p<0.05 between portal injection at 10 and 20 ml/s; c, p<0.001 between cava injection at 10 and 20 ml/s). Anterograde injection proved significant higher mean delivery index than

retrograde injection at 20 ml/s (B, p<0.01). Fig. 2C represents the intrinsic gene expression activity when perfusion was carried out at 10 ml/s, and Fig. 2D represents intrinsic gene expression activity when perfusion was carried out at 20 ml/s. The amount of eGFP DNA per cell was calculated by qPCR, and the eGFP protein per cell by ELISA. Both indexes (delivery and translation) were combined to calculate eGFP protein/gene copies ratio per cell. The intrinsic gene expression activity corresponding to each liver lobe is represented and compared. Cava vein injection achieved slightly higher intrinsic gene expression activity at both 10 and 20 ml/s, though no significant difference was observed (two-way ANOVA and Bonferroni post hoc testing). In contrast, when mean values of gene expression efficacy were compared, the 10 ml/s rate proved to succeed significantly higher mean values of intrinsic expression activity than with 20 ml/s flow rate in anterograde injection (a, p<0.05). The gene expression efficacy with retrograde perfusion at 20 ml/s rate proved to be significantly higher (B, p<0.01) than with anterograde perfusion at the same flow rate.

Figure 3. Tissue transcription index and intrinsic gene transcription activity. Two hundred ml of DNA saline solution containing the eGFP gene (20 µg/ml) was injected anterogradely (portal vein) or retrogradely (cava vein) into the liver at different flow rates (10 and 20 ml/s). Fig. 3A represents gene transcription when perfusion was carried out at 10 ml/s, and Fig. 3B represents gene transcription when perfusion was carried out at 20 ml/s. Gene transcription is indicated as eGFP copies of RNA per cell calculated by RT-qPCR, considering a total amount of RNA per cell of 20 pg. Transcription corresponding to each liver lobe is represented and compared. Retrograde injection gene transcription at 20 ml/s flow rate in lobe LM-2 was higher ***= p<0.001 than anterograde induced transcription in the same lobe and flow rate after two-way ANOVA and Bonferroni post hoc testing. The transcription induced by retrograde injection at 20 ml/s in lobe LM-2 was significantly higher ‡‡‡= p<0.001 than that induced in the same lobe with the 10 ml/s flow rate (two-way ANOVA and Bonferroni post hoc testing). Transcription index mean values of each perfusion conditions were compared statistically by nonparametric t test (Mann-Whitney correction) and retrograde perfusion proved significant higher transcription index than anterograde injection at both 10 ml/s (B, p<0.01) and 20 ml/s (C, p<0.001). Transcription index mean values of retrograde perfusion at 20 ml/s proved significant higher transcription index than at 10 ml/s (c, p<0.001). Fig. 3C represents the intrinsic activity of gene transcription when perfusion was carried out at 10 ml/s, and Fig. 3D represents gene the intrinsic activity of transcription when perfusion was carried out at 20 ml/s. The intrinsic gene transcription activity was calculated as the ratio of eGFP RNA copies per copy of eGFP DNA and cell, normalized considering the cellular RNA/DNA content. The intrinsic gene transcription activity of each liver lobe is represented and compared. No significant difference was found at 10 ml/s, although cava vein injection achieved higher intrinsic gene transcription activity (two-way ANOVA and Bonferroni post hoc testing). Intrinsic gene transcription activity induced

by retrograde injection at 20 ml/s in lobe LM-2 was significantly higher than that induced in the same lobe with the same flow direction and different flow rate (‡= p<0.05)(two-way ANOVA and Bonferroni post hoc testing). Intrinsic gene transcription activity mean value induced by retrograde injection was significantly higher than that induced with the same flow rate and different flow direction at both 10 ml/s (A= p<0.05) and 20 ml/s (C, p<0.01) (t test). The intrinsic activity of transcription mean value obtained with retrograde injection at 20 ml/s was significantly higher (a, p<0.05) than with anterograde injection at same flow rate.

Figure 4. Gene translation index and intrinsic gene translation activity. Two hundred ml of DNA saline solution containing the eGFP gene (20 µg/ml) was injected anterogradely (portal vein) or retrogradely (cava vein) into the liver at different flow rates (10 and 20 ml/s). Fig. 4A represents gene transcription when perfusion was carried out at 10 ml/s, and Fig. 4B represents gene transcription when perfusion was carried out at 20 ml/s. Gene translation is indicated as eGFP copies of protein per cell calculated by ELISA, considering a total amount of protein per cell of 0.5 ng. Translation corresponding to each liver lobe is represented; the proximal and distal samples of each lobe were combined. Ten ml/s injection gene translation was slightly higher than 20 ml/s induced translation, being significantly different (‡= p<0.05) only in lobe LM after two-way ANOVA and Bonferroni post hoc testing. The translation induced by anterograde injection at 10 ml/s rate in lobe LM was also significantly higher (*= p<0.05) than that induced in the same lobe with retrograde injection (two-way ANOVA and Bonferroni post hoc testing). Translation index mean values of each perfusion conditions were compared statistically by nonparametric t test (Mann-Whitney correction) and anterograde perfusion at 10 ml/s proved significant higher translation index than at 20 ml/s (a, p<0.05). Fig. 5C represents intrinsic activity of gene translation when perfusion was carried out at 10 ml/s, and Fig. 5D represents intrinsic activity of gene transcription when perfusion was carried out at 20 ml/s. Intrinsic gene translation activity is indicated as eGFP protein/RNA copies ratio per cell calculated by RT-qPCR (considering a total amount of RNA per cell of 20 pg) and by ELISA (considering a total protein amount per cell of 0.5 ng). Intrinsic gene translation activity corresponding to each liver lobe is represented and compared; the proximal and distal samples of each lobe were combined. Ten ml/s anterograde injection gene translation was slightly higher than 20 ml/s induced translation activity, being significantly different (‡‡‡= p<0.001) only in lobe LM after two-way ANOVA and Bonferroni post hoc testing. The translation induced by anterograde injection at 10 ml/s in lobe LM was also significantly higher (**= p<0.01) than that induced in the same lobe with retrograde injection (two-way ANOVA and Bonferroni post hoc testing). Intrinsic translation activity mean values of each perfusion conditions were compared statistically by nonparametric t test (Mann-Whitney correction) and 10 ml/s perfusion proved significant higher intrinsic translation activity than 20 ml/s rate injection with both anterograde (b, p<0.01) and retrograde (b, p<0.01) flow sense.

Figure 5. Gold nanoparticle distribution in macrophages and hepatocytes. A 200 ml citric buffer solution containing gold nanoparticles with diameters of 4 nm and 15 nm (10^{12} nanoparticles of each size per ml) was hydrodynamically injected into the liver at 20 ml/s. The left image of upper panel shows two hepatocytes and a vessel containing two macrophage cells. Boxes A and B corresponding to macrophage cells are enlarged. Large (15 nm) nanoparticles are easily visible, and 4 nm particles are referenced by black arrows. Both are located within the macrophage; the 4 nm particles are located free within the cytoplasm, while the larger nanoparticles appear to be contained in vesicles. Boxes A, B and C corresponding to hepatocyte (medium panel) cytoplasm are enlarged. Only 4 nm diameter particles are present within the hepatocyte and close to the nucleus, and are referenced by black arrows. Large (15 nm) nanoparticles are visible within vesicles in the endothelium (box D). In lower pane, the image at left shows the cytoplasm of a hepatocyte and the endothelium. Specific box A is enlarged, and different large nanoparticles are observed within the endothelial cells. Amplified specific box B shows a single large nanoparticle in the cytoplasm of the hepatocyte – this being a very infrequent event.

HEMODYNAMIC PARAMETERS

Intervention step	Cava vein injection		Portal vein injection		Global		
	Systolic Pressure (mmHg)	Diastolic Pressure (mmHg)	Systolic Pressure (mmHg)	Diastolic Pressure (mmHg)	Heart Rate (bpm)	SO2 (%)	ECG
Basal	87.3 ± 9.2	60.8 ± 6.4	98.3 ± 7.9	65.5 ± 13.4	50-60	>98	No change
Vascular exclusion							
Pre-injection	49.5 ± 3.8 ***	39.5 ± 4.8**	44.3 ± 13.8***	34.5 ± 7.1***	80-90		
End of Injection	62.5 ± 3.1**	46.3 ± 3.0	54.0 ± 5.7***	39.0 ± 1.4*	75-80	>98	No change
Pre-reperfusion	42.0 ± 5.6***	33.3 ± 3.8**	39.3 ± 5.1***	29.3 ± 5.1***	80-95		
Reperfusion							
1 min	75.5 ± 21.9‡‡	53.5 ± 20.5	82.0 ± 0.0‡‡	53.0 ± 0.0	70-80		
2 min	81.7 ± 14.6‡‡‡	57.0 ± 11.8‡	90.0 ± 0.0‡‡‡	57.0 ± 0.0	70-80	>98	No change
3 min	80.7 ± 32.3‡‡‡	67.0 ± 36.4‡‡	84.3 ± 6.7‡‡‡	53.3 ± 2.5‡	65-75		
5 min	83.0 ± 4.2‡‡‡	51.0 ± 1.4	86.8 ± 8.1‡‡‡	58.0 ± 6.3‡‡	60-70		
10 min	95.5 ± 4.9‡‡‡	59.5 ± 2.1	93.0 ± 6.2‡‡‡	59.0 ± 2.7‡‡	55-65		

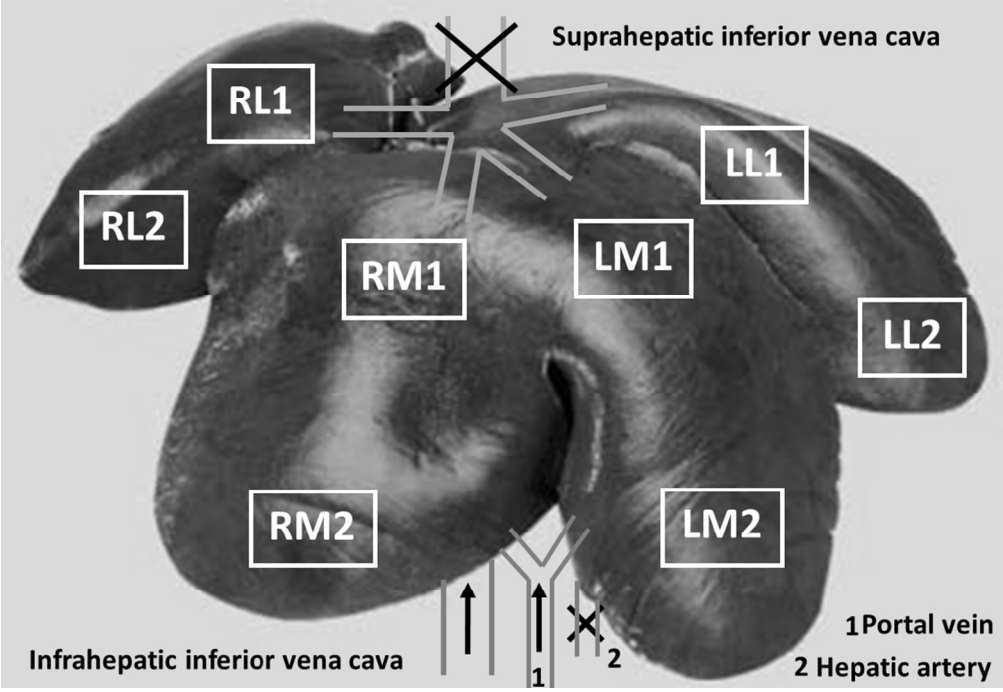

Figure 1. Surgical procedure. Schematic representation of the surgical procedure and the site of sampling. Laparotomy was performed to reference the liver vasculature. Once the vessels were referenced, suprahepatic cava vein, hepatic artery and portal or infrahepatic cava vein (depending on perfusion direction, retrograde or anterograde, respectively) were clamped to fully seal the entire liver. Then, injection was performed through the chosen vein. Tissue sampling zones are represented. The name indicates the location. First letter: R=right, L=left; second letter: M=medial, L=lateral; number: 1=proximal, 2=distal. Sampling was carried out 24 hours after injection
133x91mm (214 x 214 DPI)

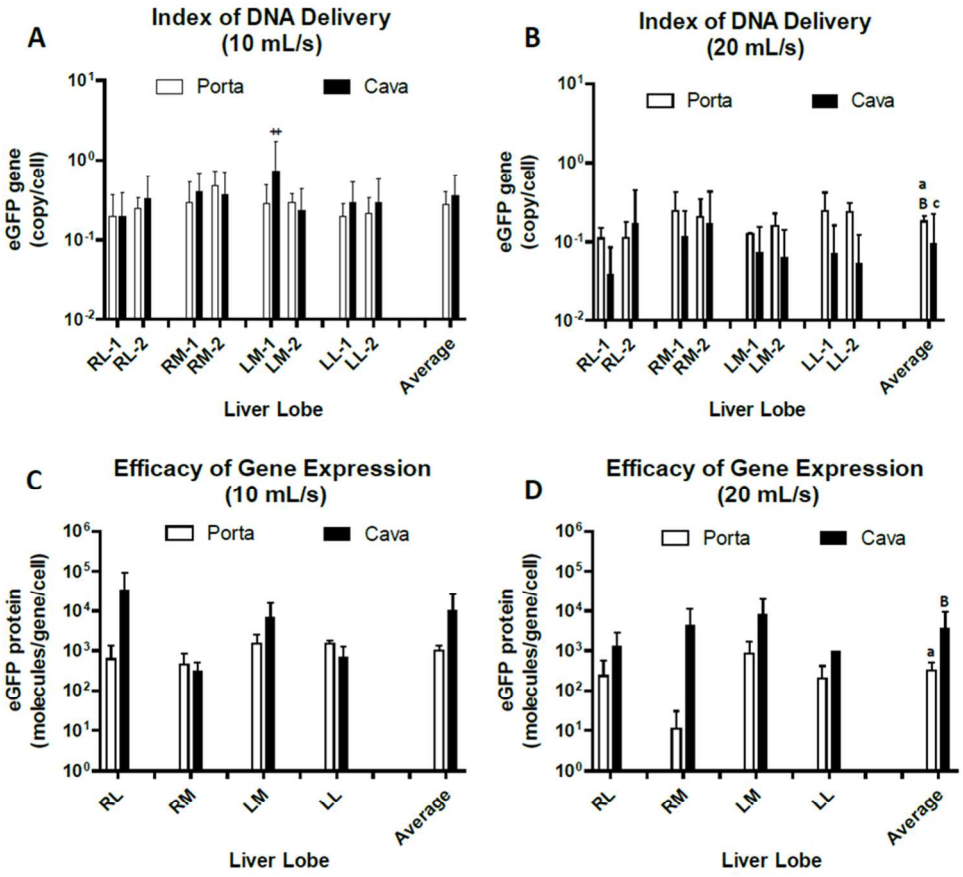

Figure 2. Gene delivery index and intrinsic gene expression activity. Two hundred ml of DNA saline solution containing the eGFP gene (20 µg/ml) was injected anterogradely (portal vein) or retrogradely (cava vein) into the liver at different flow rates (10 and 20 ml/s). Fig. 2A represents gene delivery when perfusion was carried out at 10 ml/s, Fig. 2B represents gene delivery when perfusion was carried out at 20 ml/s. Gene delivery is indicated as eGFP copies of DNA per cell calculated by qPCR, considering a pig diploid genome weight of 5.4 pg. Delivery corresponding to each liver lobe is represented. Portal vein injection achieved similar gene delivery at 10 ml/s and slightly higher gene delivery at 20 ml/s, significant difference was observed for LM-1 lobe retrogradely injected at 10 ml/s (marked with ǂ, $p<0.5$) (two-way ANOVA and Bonferroni post hoc testing). Delivery index mean values of every perfusion condition were compared statistically by nonparametric (Mann-Whitney correction) t test and results showed significant differences between different flow rates and same flow direction (a, $p<0.5$ between portal injection at 10 and 20 ml/s; c, $p<0.001$ between cava injection at 10 and 20 ml/s). Anterograde injection proved significant higher mean delivery index than retrograde injection at 20 ml/s (B, $p<0.01$). Fig. 2C represents the intrinsic gene expression activity when perfusion was carried out at 10 ml/s, and Fig. 2D represents intrinsic gene expression activity when perfusion was carried out at 20 ml/s. The amount of eGFP DNA per cell was calculated by qPCR, and the eGFP protein per cell by ELISA. Both indexes (delivery and translation) were combined to calculate eGFP protein/gene copies ratio per cell. The intrinsic gene expression activity corresponding to each liver lobe is represented and compared. Cava vein injection achieved slightly higher intrinsic gene expression activity at both 10 and 20 ml/s, though no significant difference was observed (two-way ANOVA and Bonferroni post hoc testing). In contrast, when mean values of gene expression efficacy were compared, the 10 ml/s rate proved to succeed significantly higher mean values of intrinsic expression activity than with 20 ml/s flow rate in anterograde injection (a, $p<0.5$). The gene expression efficacy with retrograde perfusion at 20 ml/s rate proved to be significantly higher (B, $p<0.01$) than with

anterograde perfusion at the same flow rate.
202x189mm (127 x 127 DPI)

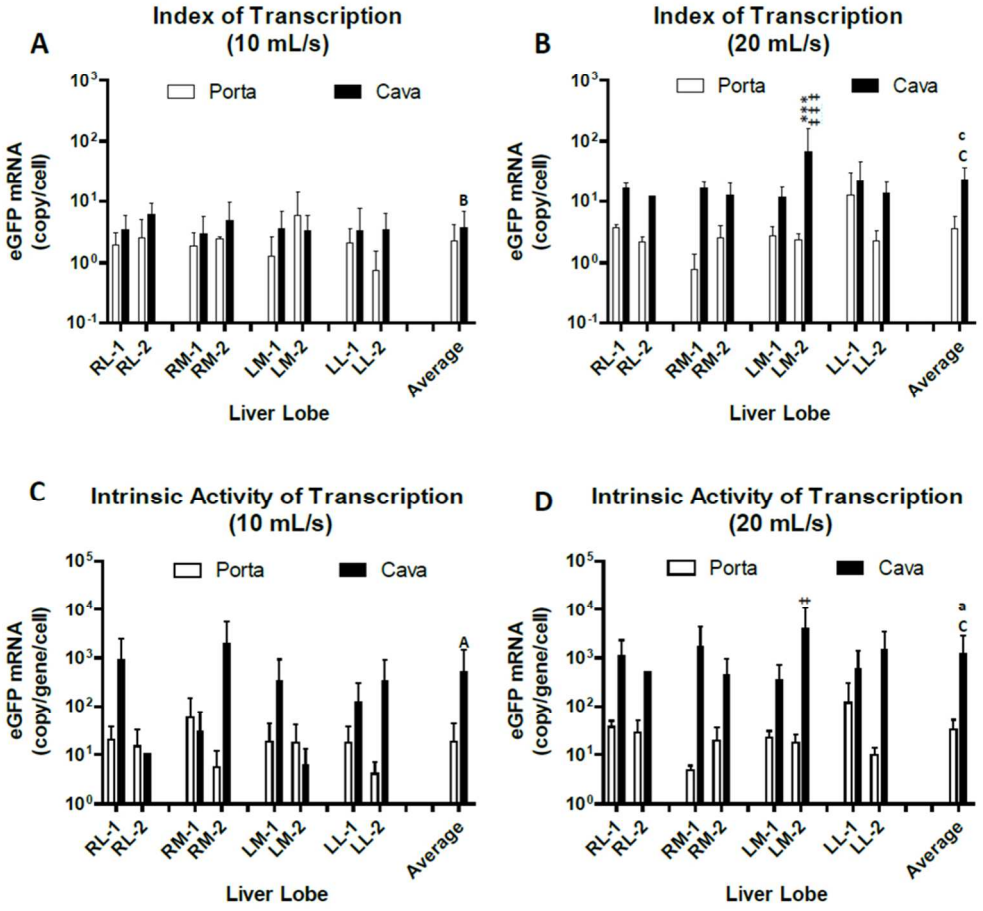

Figure 3. Tissue transcription index and intrinsic gene transcription activity. Two hundred ml of DNA saline solution containing the eGFP gene (20 µg/ml) was injected anterogradely (portal vein) or retrogradely (cava vein) into the liver at different flow rates (10 and 20 ml/s). Fig. 3A represents gene transcription when perfusion was carried out at 10 ml/s, and Fig. 3B represents gene transcription when perfusion was carried out at 20 ml/s. Gene transcription is indicated as eGFP copies of RNA per cell calculated by RT-qPCR, considering a total amount of RNA per cell of 20 pg. Transcription corresponding to each liver lobe is represented and compared. Retrograde injection gene transcription at 20 ml/s flow rate in lobe LM-2 was higher ***= $p<0.001$ than anterograde induced transcription in the same lobe and flow rate after two-way ANOVA and Bonferroni post hoc testing. The transcription induced by retrograde injection at 20 ml/s in lobe LM-2 was significantly higher ‡‡‡= $p<0.001$ than that induced in the same lobe with the 10 ml/s flow rate (two-way ANOVA and Bonferroni post hoc testing). Transcription index mean values of each perfusion conditions were compared statistically by nonparametric t test (Mann-Whitney correction) and retrograde perfusion proved significant higher transcription index than anterograde injection at both 10 ml/s (B, $p<0.01$) and 20 ml/s (C, $p<0.001$). Transcription index mean values of retrograde perfusion at 20 ml/s proved significant higher transcription index than at 10 ml/s (c, $p<0.001$). Fig. 3C represents the intrinsic activity of gene transcription when perfusion was carried out at 10 ml/s, and Fig. 3D represents gene the intrinsic activity of transcription when perfusion was carried out at 20 ml/s. The intrinsic gene transcription activity was calculated as the ratio of eGFP RNA copies per copy of eGFP DNA and cell, normalized considering the cellular RNA/DNA content. The intrinsic gene transcription activity of each liver lobe is represented and compared. No significant difference was found at 10 ml/s, although cava vein injection achieved higher intrinsic gene transcription activity (two-way ANOVA and Bonferroni post hoc testing). Intrinsic gene transcription activity induced by retrograde injection at 20 ml/s in lobe LM-2 was significantly

higher than that induced in the same lobe with the same flow direction and different flow rate (‡= p<0.05)(two-way ANOVA and Bonferroni post hoc testing). Intrinsic gene transcription activity mean value induced by retrograde injection was significantly higher than that induced with the same flow rate and different flow direction at both 10 ml/s (A= p<0.05) and 20 ml/s (C, p<0.01) (t test). The intrinsic activity of transcription mean value obtained with retrograde injection at 20 ml/s was significantly higher (a, p<0.05) than with anterograde injection at same flow rate.
199x190mm (127 x 127 DPI)

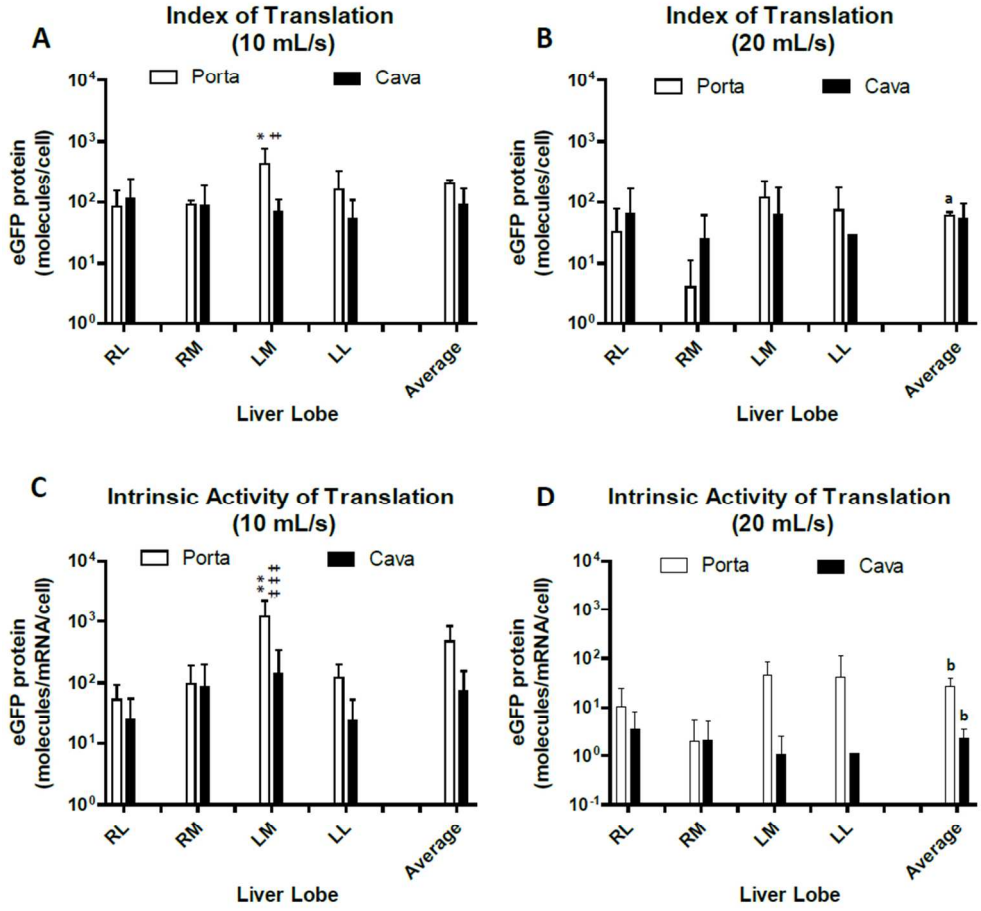

Figure 4. Gene translation index and intrinsic gene translation activity. Two hundred ml of DNA saline solution containing the eGFP gene (20 µg/ml) was injected anterogradely (portal vein) or retrogradely (cava vein) into the liver at different flow rates (10 and 20 ml/s). Fig. 4A represents gene transcription when perfusion was carried out at 10 ml/s, and Fig. 4B represents gene transcription when perfusion was carried out at 20 ml/s. Gene translation is indicated as eGFP copies of protein per cell calculated by ELISA, considering a total amount of protein per cell of 0.5 ng. Translation corresponding to each liver lobe is represented; the proximal and distal samples of each lobe were combined. Ten ml/s injection gene translation was slightly higher than 20 ml/s induced translation, being significantly different (‡= $p<0.05$) only in lobe LM after two-way ANOVA and Bonferroni post hoc testing. The translation induced by anterograde injection at 10 ml/s rate in lobe LM was also significantly higher (*= $p<0.05$) than that induced in the same lobe with retrograde injection (two-way ANOVA and Bonferroni post hoc testing). Translation index mean values of each perfusion conditions were compared statistically by nonparametric t test (Mann-Whitney correction) and anterograde perfusion at 10 ml/s proved significant higher translation index than at 20 ml/s (a, $p<0.05$). Fig. 5C represents intrinsic activity of gene translation when perfusion was carried out at 10 ml/s, and Fig. 5D represents intrinsic activity of gene transcription when perfusion was carried out at 20 ml/s. Intrinsic gene translation activity is indicated as eGFP protein/RNA copies ratio per cell calculated by RT-qPCR (considering a total amount of RNA per cell of 20 pg) and by ELISA (considering a total protein amount per cell of 0.5 ng). Intrinsic gene translation activity corresponding to each liver lobe is represented and compared; the proximal and distal samples of each lobe were combined. Ten ml/s anterograde injection gene translation was slightly higher than 20 ml/s induced translation activity, being significantly different (‡‡‡= $p<0.001$) only in lobe LM after two-way ANOVA and Bonferroni post hoc testing. The translation induced by anterograde injection at 10 ml/s in lobe LM was also significantly higher (**= $p<0.01$) than that

induced in the same lobe with retrograde injection (two-way ANOVA and Bonferroni post hoc testing). Intrinsic translation activity mean values of each perfusion conditions were compared statistically by nonparametric t test (Mann-Whitney correction) and 10 ml/s perfusion proved significant higher intrinsic translation activity than 20 ml/s rate injection with both anterograde (b, $p<0.01$) and retrograde (b, $p<0.01$) flow sense.
197x190mm (128 x 128 DPI)

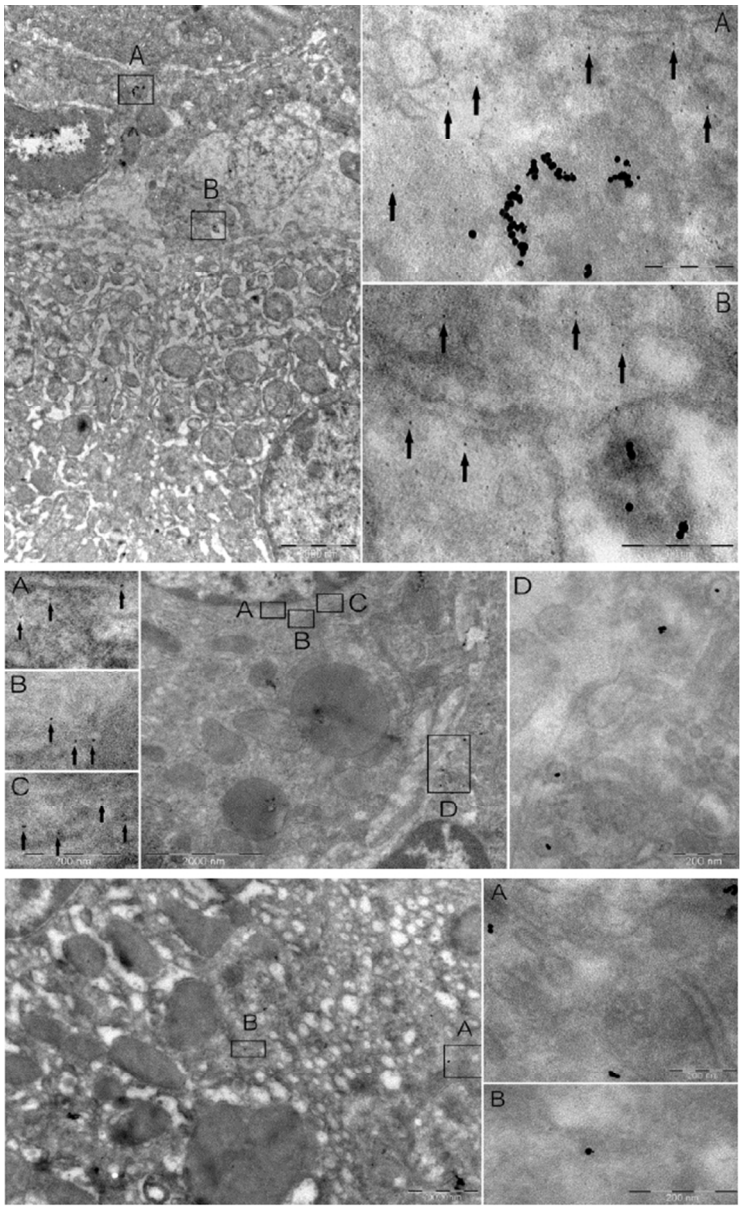

Figure 5. Gold nanoparticle distribution in macrophages and hepatocytes. A 200 ml citric buffer solution containing gold nanoparticles with diameters of 4 nm and 15 nm (1012 nanoparticles of each size per ml) was hydrodynamically injected into the liver at 20 ml/s. The left image of upper panel shows two hepatocytes and a vessel containing two macrophage cells. Boxes A and B corresponding to macrophage cells are enlarged. Large (15 nm) nanoparticles are easily visible, and 4 nm particles are referenced by black arrows. Both are located within the macrophage; the 4 nm particles are located free within the cytoplasm, while the larger nanoparticles appear to be contained in vesicles. Boxes A, B and C corresponding to hepatocyte (medium panel) cytoplasm are enlarged. Only 4 nm diameter particles are present within the hepatocyte and close to the nucleus, and are referenced by black arrows. Large (15 nm) nanoparticles are visible within vesicles in the endothelium (box D). In lower pane, the image at left shows the cytoplasm of a hepatocyte and the endothelium. Specific box A is enlarged, and different large nanoparticles are observed within the endothelial cells. Amplified specific box B shows a single large nanoparticle in the cytoplasm of the hepatocyte – this being a very infrequent event.

1
2
3
4
5
6
7
8
9
10
11
12
13
14
15
16
17
18
19
20
21
22
23
24
25
26
27
28
29
30
31
32
33
34
35
36
37
38
39
40
41
42
43
44
45
46
47
48
49
50
51
52
53
54
55
56
57
58
59
60

165x269mm (96 x 96 DPI)

Enzyme	Sampling Time (h)	Injection Vein		Normal values
		Portal	Cava	
AST	**0**	40.7 ± 13.2	39.2 ± 10.6	
(U/l)	**1**	91.7 ± 16.6	72.4 ± 29.9	**15-55 UI**
	24	82.3 ± 60.7	37.4 ± 11.5	
ALT	**0**	29.7 ± 4.0	30.4 ± 4.5	
(U/l)	**1**	35.3 ± 2.3	32.8 ± 3.4	**21-46 UI**
	24	41.0 ± 14.0	36.8 ± 7.8	